Crystalline mono- and multilayer self-assemblies of oligothiophenes at the air–water interface

Sandrine Isz, Isabelle Weissbuch, Kristian Kjaer, Wim G. Bouwman, Jens Als-Nielsen, Serge Palacin, Annie Ruaudel-Teixier, Leslie Leiserowitz,* and Meir Lahav*

Dedicated to the memory of Dr. Lev Margulis

Abstract: The formation of Langmuir monolayers at the air–water interface has long been believed to be limited to amphiphilic molecules containing a hydrophobic chain and a hydrophilic headgroup. Here we report the formation of crystalline mono- and multilayer self-assemblies of oligothiophenes, a class of aromatic nonamphiphilic molecules, self-aggregated at the air–water interface. As model systems we have examined the deposition of quaterthiophene (S_4), quinquethiophene (S_5), and sexithiophene (S_6) from chloroform solutions on the water surface. The structures of the films were determined by surface pressure–area isotherms, by scanning force microscopy (SFM) after transfer of the films onto atomically smooth mica, by cryo-transmission electron microscopy (Cryo-TEM) on vitreous ice, and by grazing incidence synchrotron X-ray diffraction (GID) directly on the water surface. S_4 forms two polymorphic crystalline multilayers. In polymorph α, of structure very similar to that of the three-dimensional solid, the molecules are aligned with their long molecular axis tilted by about 23° from the normal to the water surface. In polymorph β the long molecular axis is perpendicular to the water surface. S_5 self-aggregates at the water surface to form mixtures of monolayers and bilayers of the β polymorph; S_6 forms primarily crystalline monolayers of both α and β forms. The crystalline assemblies preserve their integrity during transfer from the water surface onto solid supports. The relevance of the present results for the understanding of the early stages of crystal nucleation is presented.

Keywords
cryo-transmission electron microscopy · monolayers · oligothiophenes · polymorphism · scanning force microscopy

Introduction

Polythiophenes are currently attracting attention owing to their physical properties as processable polymeric organic conductors.[1, 2] These molecules have also been used as molecular wires inside Langmuir–Blodgett films to induce charge transfer between donors and acceptors.[3] Since these physical properties depend upon the structure and the orientation of the molecules in a solid matrix,[4, 5] the construction of thin organic films by techniques such as Langmuir–Blodgett or self-assembly is of great interest.

Recent studies have demonstrated that hydrophobic molecules such as *n*-perfluoroalkanes[6] and *n*-alkanes,[7] upon deposition on a water surface, form crystalline self-aggregates akin to those formed by amphiphilic molecules bearing polar headgroups. In order to probe the generality of the crystalline film formation by hydrophobic molecules, we embarked upon an analysis of the packing arrangements of polyaromatic molecules on the water surface. Here we describe structural studies on the self-organization of oligothiophenes by surface pressure–area isotherms and grazing incidence X-ray diffraction (GID) on a water surface, by scanning force microscopy (SFM) after deposition onto a smooth mica surface, and by cryo-transmission electron microscopy (Cryo-TEM) on vitreous ice. The ability to determine the structure of the uncompressed oligothiophene self-assemblies on water and after transfer to a solid support provides a better way of monitoring the film properties.

Experimental Section

Quaterthiophene (S_4) and quinquethiophene (S_5) were synthesized from dibromothiophene and dibromobithiophene, respectively, by means of a modified Steinkopf method[8] with a phosphine–nickel complex catalyst. Sexithiophene (S_6) was synthesized from terthiophene by means of an oxidative coupling procedure involving $CuCl_2$.[9]

[*] M. Lahav, L. Leiserowitz, S. Isz, I. Weissbuch
Department of Materials and Interfaces, Weizmann Institute of Science
Rehovot 76100 (Israel)
Fax: Int. code +(8)934-4138
e-mail: bpherut@weizmann.weizmann.ac.il

S. Palacin, A. Ruaudel-Teixier
Service de Chimie Moléculaire, DRECAM, CEA Saclay
F-91191 Gif sur Yvette (France)

K. Kjaer, W. G. Bouwman
Department of Solid State Physics, Risø National Laboratory
DK-4000 Roskilde (Denmark)

J. Als-Nielsen
H. C. Ørsted Laboratory, Niels Bohr Institute
Universitetsparken 5, DK-2100 Copenhagen (Denmark)

0947-6539/97/0306-0930 $ 17.50+.50/0

Surface pressure–area (π–A) isotherms of the materials dissolved in pure chloroform (Merck) were measured on a Lauda trough at room temperature.

Scanning force microscopy (SFM) measurements were performed in air with a Topometrix TMX 2010 stage. Sample preparation involved spreading of the solution on the water surface, for a nominal area per molecule of 25 Å^2, at room temperature, followed by cooling to 5 °C. The subphase was then slowly drained in order to deposit the film onto a freshly cleaved mica support located below the water level.[10]

Cryo-transmission electron microscopy (Cryo-TEM) measurements were performed on a Philips CM 12 microscope with collodion-carbon coated 400 mesh grids mounted on a Gatan cold stage for work at −175 °C. The samples were prepared in a manner similar to that of SFM, but transferred onto the electron microscope grids. After film transfer the grids were plunged into liquid ethane to vitrify the water layer.[11]

Grazing incidence X-ray diffraction (GID) experiments were carried out on the liquid surface diffractometer at the synchrotron beamline BW1, Hasylab, DESY, Hamburg. The experimental setup has been described elsewhere.[12, 13] The oligothiophene samples for the GID experiments were prepared by spreading solutions in various concentrations that were freshly sonicated or had been aged for about one day onto the water surface at room temperature. After spreading for a given nominal area per molecule, the samples were cooled to 5 °C and GID measurements were performed at various points along the isotherm.

In a GID experiment the evanescent wave is diffracted by the lateral 2D crystalline order, leading to Bragg peaks in the measurement of scattered intensity as a function of the horizontal component (q_{xy}) of the scattering vector. There is no restriction on the vertical component (q_z) of the Bragg scattered beam leading to so-called Bragg rods. With a Soller collimator to define the horizontal scattering angle $2\theta_{xy}$ and a vertical position-sensitive detector to define the vertical scattering angle α_f, where α_f is the angle between the water surface and the scattered beam, one thus determines the horizontal (q_{xy}) as well as the vertical (q_z) components of the scattering vector. The term q_{xy} is approximately equal to $(4\pi/\lambda)\sin(\theta_{xy})$. The vertical component q_z is equal to $(2\pi/\lambda)\sin\alpha_f$. The q_{xy} values yield the unit cell dimensions, and the intensity distribution along q_z permits determination of the molecular packing. The GID data of the mono- and multilayers were analysed in terms of unit cell dimensions and plane group (or space group) determination as well as X-ray structure factor calculations with atomic coordinate models to fit the Bragg rod intensity profiles, as described elsewhere.[14]

Results

Surface–pressure isotherms: The solubility of the oligothiophenes (S_n, $n = 4$–6, Scheme 1) in organic solvents decreases with an increase of the number of thiophene rings. Quaterthiophene (S_4) was spread on the water surface from solutions of various concentrations (0.5 mM, 25 μM, 7 μM). The isotherms became more expanded with increasing dilution (Figure 1a), but also with sonication. The nominal area per molecule (i.e., trough surface area divided by the number of molecules) of the compressed film varies from 5 to 10 Å^2 with dilution. These values suggest that the molecules mainly form multilayers.

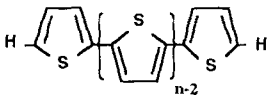

Scheme 1. Oligothiophenes S_n, $n = 4, 5, 6$.

S_5 and S_6, being less soluble, were spread from very dilute solutions, for example 7 μM. These two oligomers show similar isotherms with a limiting area per molecule of about 25 Å^2 (Figure 1b, curves b and c), indicating monolayer formation in which the long molecular axes are aligned perpendicular to the water surface.

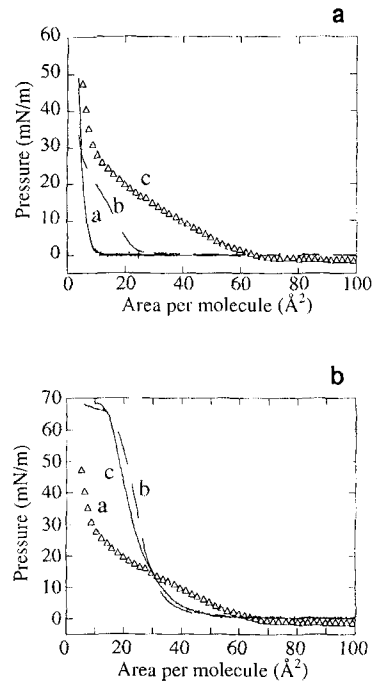

Figure 1. a) Surface pressure–area isotherms of S_4 spread from $CHCl_3$ solutions at various concentrations (a, —: 0.5 mM; b, – –: 25 μM; c, △: 7 μM); b) surface pressure–area isotherms of oligothiophenes (a, △: S_4; b, – –: S_5; c, —: S_6) spread from 7 μM $CHCl_3$ solutions.

Scanning force microscopy (SFM): In order to obtain further knowledge on the structure and size of these assemblies, we transferred the films from the water surface onto atomically smooth mica by draining the water, and analysed them by SFM.[15]

Figure 2a shows a SFM topography image of S_4 on mica obtained from a 0.5 mM solution. The observed domains are heterogeneous and rounded in shape. The measured thickness in different regions of the sample varies from 60 to 200 Å. On spreading from dilute solution (7 μM), the domains became much larger in size and much thinner (16 Å), as shown in Figure 2b. SFM studies performed on S_5 reveal the formation of large areas (2–5 μm) of monolayer, 20 Å thick (shown in Figure 2c), and several multilayer domains (not shown). S_6 forms a monolayer film with a thickness of 26 Å (Figure 2d). These film thicknesses of 16, 20, and 26 Å for S_4, S_5, and S_6 respectively, which correspond to their molecular lengths, indicate that the molecules preserve their orientation after transfer from the water surface onto the mica support.

Cryo-transmission electron microscopy (Cryo-TEM): We studied films on vitreous ice by Cryo-TEM in order to glean information on their crystallinity and morphology. The bright field images of S_4 shown in Figure 3a display round domains similar to those observed by SFM. Differences of contrast were observed in different areas of the sample, which presumably correspond to the formation of layers of different thickness. On the other hand, the electron microscopy bright field images for S_5 and S_6 are somewhat different; S_6 forms a homogeneous film (Figure 3g) whereas the film formed by S_5 is inhomogeneous (Figure 3d).

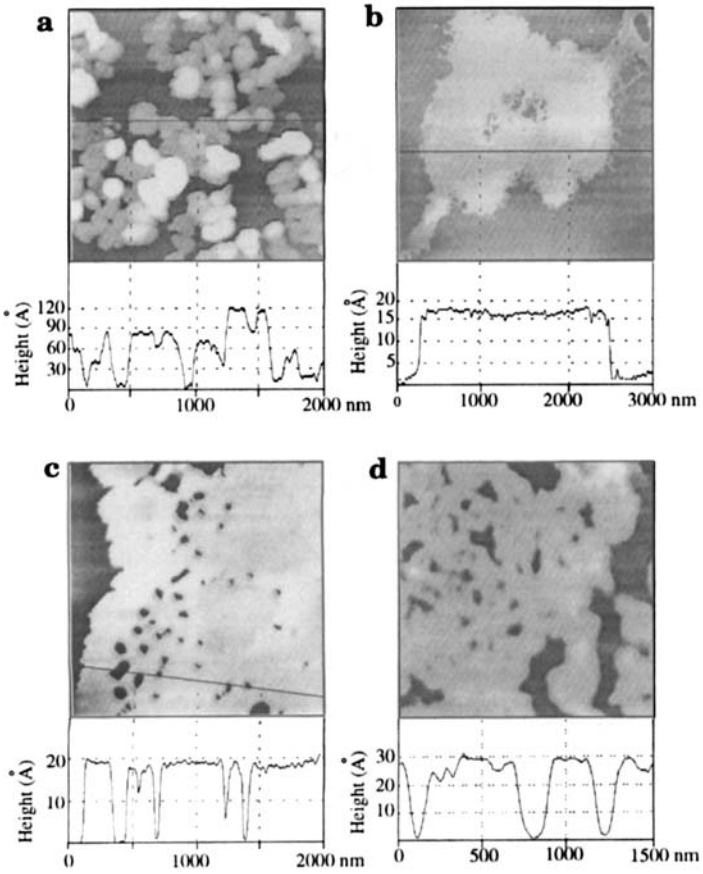

Figure 2. SFM topography images and height profiles of: a) S_4 film obtained from a concentrated solution (0.5 mM); b) S_4 film obtained from a dilute solution (7 μM); c) S_5 film obtained from a dilute solution (7 μM); d) S_6 film obtained from a dilute solution (7 μM).

The electron diffraction pattern of the S_4 crystallites is shown in Figure 3b. The intense spots from a single crystal, superimposed on rings, reveal a preferential orientation. The spots with the largest *d*-spacings of 4.3, 3.75, 3.08 Å were assigned Miller *(h,k)* indices (1,1), (0,2), and (1,2) respectively, yielding a rectangular unit cell of dimensions $a = 5.4$ and $b = 7.5$ Å. Based on this unit cell, the additional higher-order reflections could be indexed (Figure 3c). The observed rings indicate the presence of an additional phase with *d*-spacings of 4.6, 3.8, and 3.1 Å, which were assigned *(h,k)* indices (1,1), (0,2), and (1,2), yielding a rectangular cell of dimensions $a = 5.8$ and $b = 7.6$ Å. This result shows the presence of two polymorphs, α and β.

The electron diffraction patterns of S_5 include three strong diffraction rings of *d*-spacings 4.60, 3.90, 3.25 Å (Figure 3e); the corresponding bright field image is shown in Figure 3d. The electron diffraction pattern of S_6 arises from a single crystal (Figure 3h), and thus could be unambiguously indexed (Figure 3i). Rectangular unit cells of dimensions $a = 5.6$, $b = 7.6$ Å for S_5 and $a = 5.7$, $b = 7.9$ Å for S_6 were derived. The calculated area per molecule (*ab*/2) for each crystallite is 21.3 and 22.3 Å^2, respectively.

Grazing incidence X-ray diffraction (GID): The surface diffraction measurements provide direct information on the crystallinity and structure of the films on the water surface. Moreover it is possible to derive their crystal structures to near-atomic resolution.

Quaterthiophene S_4: As previously described, S_4 yielded a π-*A* isotherm of a shape dependent on the concentration and sonication time of the spreading solutions, and therefore we investigated the effect of these parameters on the structure and thickness of the S_4 films in situ on the water surface. First we measured the GID patterns of S_4 samples formed by spreading a 0.47 mM chloroform solution that was sonicated for 2 hours, or aged for one day just before use. The GID measurements were performed for various nominal areas per molecule. The sample prepared by spreading the freshly sonicated solution yielded a highly intense GID pattern at nominal areas per molecule of 25 and 17 Å^2. In contrast, the sample prepared by spreading the aged solution did not diffract at an area per molecule of 25 Å^2, but a GID pattern was obtained for 12.5 Å^2, at which point the surface pressure just began to rise (Figure 1). The three GID patterns are very similar and consist of six major Bragg peaks, shown in Figure 4a.

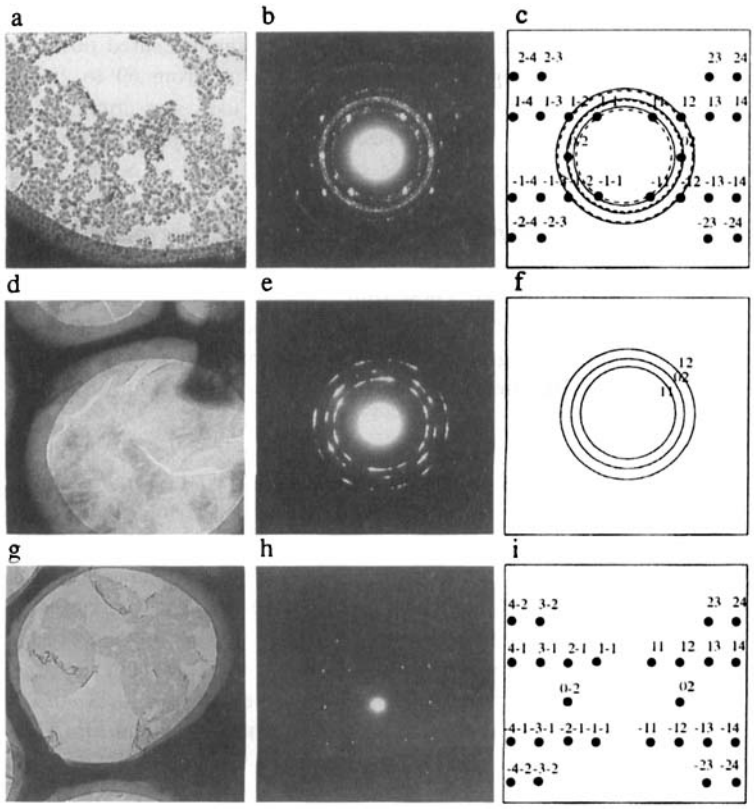

Figure 3. a, d, g) Cryo-transmission electron microscopy bright field images corresponding to the S_4, S_5, and S_6 films, respectively (scale: 6.5 mm = 1.5 μm for a and g; 6.5 mm = 2.4 μm for d); b, e, h) observed electron diffraction patterns of S_4, S_5, and S_6 films, respectively; c, i) drawings of the Miller-indexed reciprocal lattices of the electron diffraction patterns b and h, respectively. Note that in c the solid circles (powder diffraction) and the intense spots (from a single crystal) superimposed correspond to the β polymorph. The powder lines arising from the α polymorph are dashed. f) Indexed powder pattern corresponding to e.

0947-6539/97/0306-0932 $ 17.50+.50/0 Chem. Eur. J. 1997, 3, No. 6

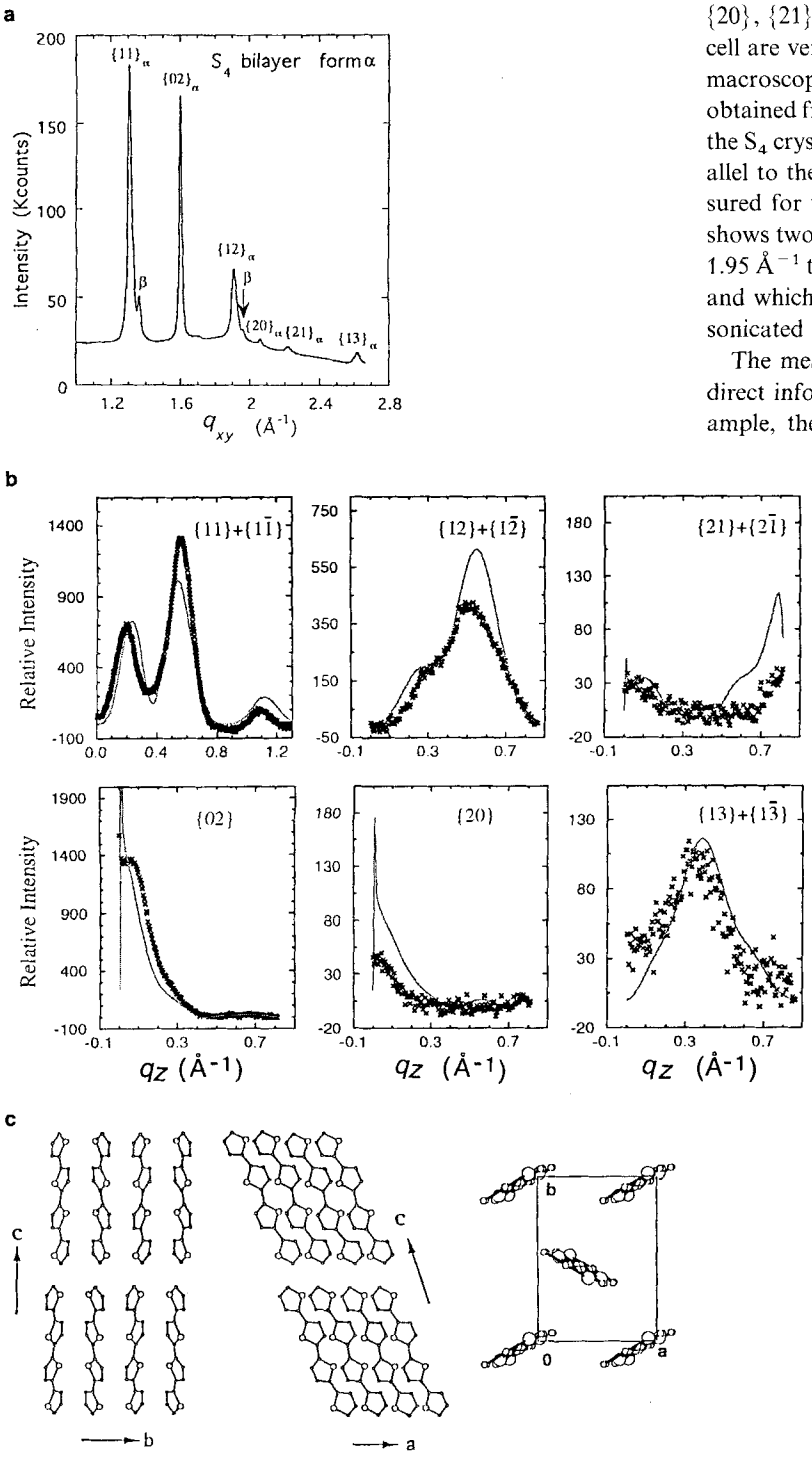

Figure 4. GID results for the Langmuir film of S_4 prepared from a spreading solution of 0.5 mM. a) Total scattered intensity $I(q_{xy})$ as a function of the horizontal q_{xy} component of the scattering vector q. The two reflections corresponding to a minor phase are denoted as β; b) measured ($\times\times$) and calculated (—) Bragg rod intensity profiles $I(q_z)$ of the reflections $\{11\}+\{1\bar{1}\}$, $\{02\}$, $\{20\}$, $\{12\}+\{1\bar{2}\}$, $\{21\}+\{2\bar{1}\}$, and $\{13\}+\{1\bar{3}\}$; c) left, middle: crystalline packing arrangement of the bilayer viewed parallel to the water surface (along the a and b axes respectively); right: layer packing viewed parallel to the long molecular axis.

Assignment of the two peaks at q_{xy} values of 1.31 and 1.60 Å^{-1} with Miller indices $\{11\}+\{1\bar{1}\}$ and $\{02\}$, respectively, yielded a rectangular cell of dimensions $a = 6.08$, $b = 7.86$ Å and a molecular area of 23.9 Å^2. Corresponding to this cell, an additional four observed reflections were assigned indices $\{12\}+\{1\bar{2}\}$, $\{20\}$, $\{21\}+\{2\bar{1}\}$, and $\{13\}+\{1\bar{3}\}$. The dimensions of this 2D cell are very similar to those reported for the layer structure in macroscopic S_4 powders, the packing arrangement of which was obtained from X-ray powder diffraction data.[16] Consequently, the S_4 crystallites must consist of molecular layers oriented parallel to the water surface. Inspection of the GID pattern measured for the sample prepared by spreading the aged solution shows two additional very weak peaks at q_{xy} values of 1.36 and 1.95 Å^{-1} that correspond to a different polymorph (Figure 4a), and which were not observed for the film spread from freshly sonicated solution.

The measured Bragg rod intensity profiles (Figure 4b) give direct information on the thickness of the crystallites. For example, the $\{11\}+\{1\bar{1}\}$ intensity profile displays modulations with a full width at half maximum (FWHM = 0.17 Å^{-1}) yielding an estimated film thickness of about 33 Å.[17] The separation (Δq_z = 0.37 Å^{-1}) between the first two modulations at $q_z \approx 0.19$ Å^{-1} and $q_z \approx 0.56$ Å^{-1} indicates an interlayer spacing of about 17 Å ($= 2\pi/0.37$). Therefore the crystallites consist of two layers.[18]

A detailed packing structure of S_4 crystallites was obtained by X-ray structure factor calculations for a molecular model constructed from the 3D single crystal structure of S_6.[19] The resulting calculated Bragg rod intensity profiles compare reasonably well with the measured values (Figure 4b). The packing arrangement, shown in Figure 4c, consists of a bilayer with the molecules related by twofold screw symmetry (along the b axis) within the layer. The second layer is generated across a center of inversion, as in the 3D single crystal of S_6. The molecular axis makes an angle of 23.5° with the normal to the layer plane. We may express this bilayer structure in terms of a unit cell $a = 6.08$, $b = 7.86$, $c = 15.5$ Å, $\beta = 101°$, space group $P2_1/a$, with two molecules in the cell and whose centers coincide with the crystallographic inversion centers.

We now focus on the effect of concentration of the spreading solution. The GID measurements were performed on S_4 samples prepared from a freshly sonicated (3 hours), very dilute solution (6.8 μM) spread for a nominal area per molecule of 50 Å^2. Diffraction patterns were measured at 25 and 17 Å^2 per molecule. The resulting GID pattern (Figure 5a) is displayed in the form of a two-dimensional intensity distribution $I(q_{xy},q_z)$ as a function of the horizontal (q_{xy}) and vertical (q_z) components of the scattering vector q. The three Bragg peaks at q_{xy} values of 1.37, 1.64, and 1.95 Å^{-1} were assigned Miller indices $\{11\}+\{1\bar{1}\}$, $\{02\}$ and $\{12\}+\{1\bar{1}\}$, yielding a 2D rectangular cell of dimensions $a = 5.71$, $b = 7.67$ Å and an area per molecule of 21.9 Å^2. This polymorph, which was observed also for S_4 spread from concentrated solution but as a minor phase, will be denoted as the β form, since it was not reported for the macroscopic solid (α polymorph).

The ab unit cell dimensions of the α form, when projected onto a plane perpendicular to the long molecular axis, yield axes $a_p = 5.58$ Å ($= a\cos t$, where t is the molecular tilt angle of 23.5° along the a axis), $b_p = b = 7.86$ Å. The molecular cross-sectional area $a_p b_p/2 = 21.9$ Å^2 matches the molecular area of the β form. These results indicate that in this β form the molecular axis must be almost perpendicular to the layer plane. Furthermore, the agreement between the lengths of the corresponding axes a_p, b_p of the α form and a, b of the β form is fingerprint evidence that the two molecules within the layer must be related by glide symmetry in the same way as in the α form. The only remaining question is the symmetry and spatial relation between the two layers. The interlayer contacts in the 3D crystal structures of oligothiophenes S_6[19] and S_8[20] are achieved across centers of inversion. The same symmetry operation was assumed for the interlayer arrangement of the β form. The layer symmetry is $2_1/a$, where the 2_1 axis is parallel to b and the glide is along the a axis. In order to maintain this $2_1/a$ crystallographic symmetry for the bilayer, the two layers related by translation can be offset only along the a axis. We obtained an excellent fit between the calculated and observed (Figure 5b) *positions* of the Bragg rod maxima for an interlayer spacing of 17.4 Å and an offset between the translationally related layers of 2.1 Å in the direction of the a axis (Figure 5c). The poor agreement between the observed and calculated *intensity* profiles, particularly for the {1,2} reflection, is most likely due to X-ray beam damage to the sample. The skewed peak at q_{xy} 1.47 Å^{-1} (Figure 5a) must belong to an unknown crystalline phase or to an impurity (see results for S_5).

In conclusion, S_4 crystalline self-assemblies on water display polymorphism dependent on the concentration of the spreading solution. The samples prepared from relatively concentrated spreading solutions crystallize in the α polymorph as the major phase, with molecules tilted from the layer normal by 23.5°, whereas the samples prepared from very dilute spreading solutions crystallize in a β polymorph with molecules aligned normal to the layer plane.

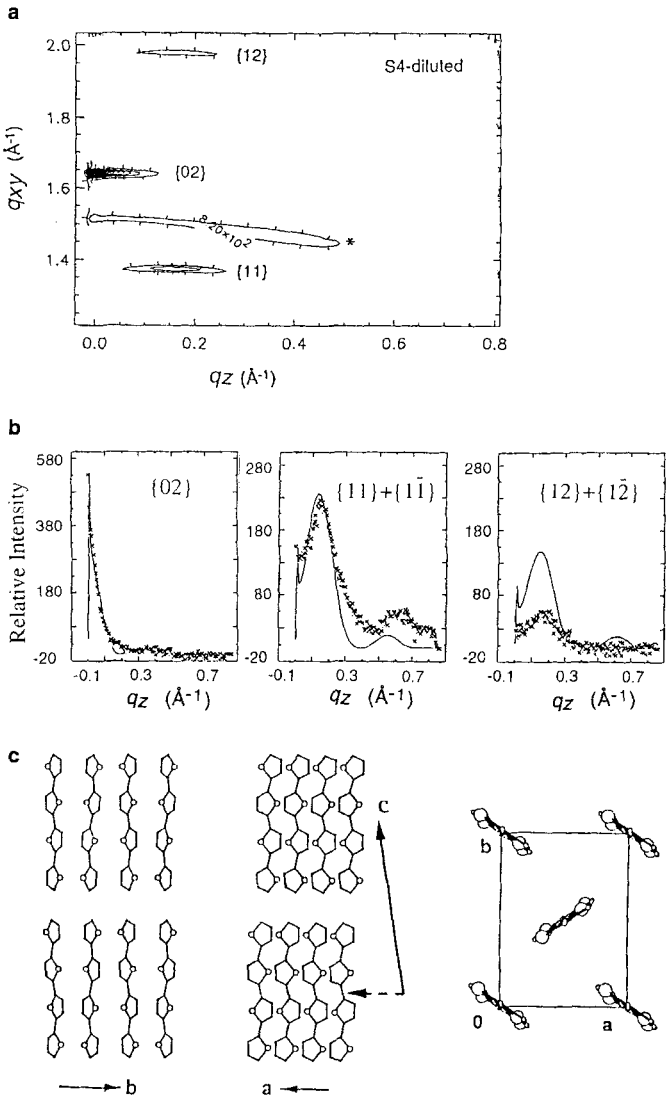

Figure 5. GID results for the film of S_4 prepared from a spreading solution of 6.8 μM. a) Two-dimensional scattered intensity contour plot $I(q_{xy}, q_z)$ as a function of the horizontal q_{xy} and vertical q_z components of the total scattering vector q; b) measured (× ×) and calculated (—) Bragg rod intensity profiles $I(q_z)$ of the reflections $\{11\}+\{1\bar{1}\}$, $\{02\}$, and $\{12\}+\{1\bar{2}\}$; c) left, middle: crystalline packing arrangement of the bilayer viewed parallel to the water surface (along the a and b axes, respectively); right: layer packing viewed perpendicular to the water surface.

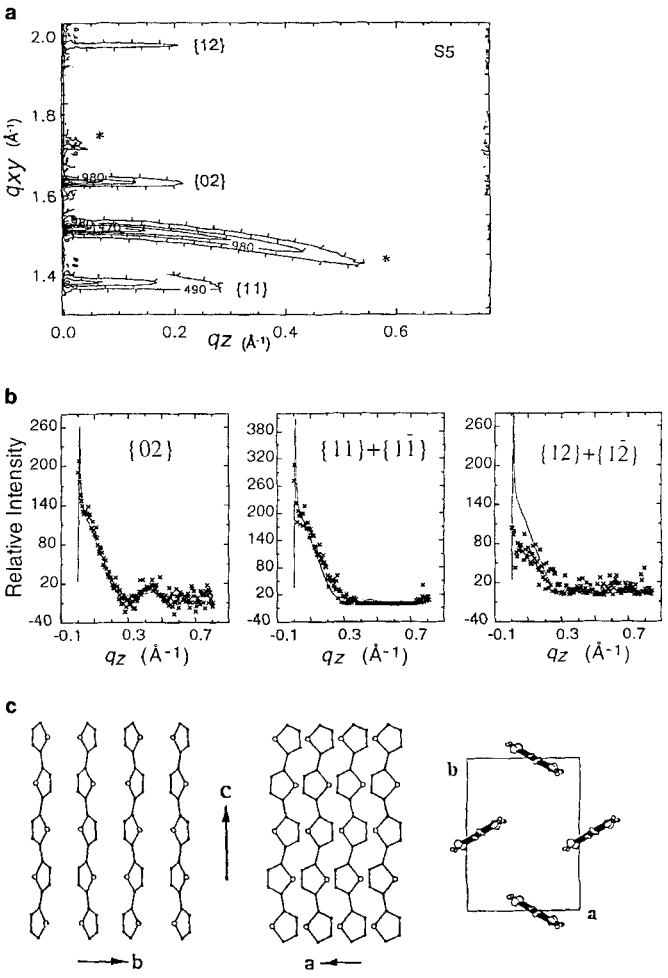

Figure 6. GID results for a monolayer film of S_5 prepared from a spreading solution of 6.8 μM. a) Two-dimensional scattered intensity contour plot $I(q_{xy}, q_z)$ as a function of the horizontal q_{xy} and vertical q_z components of the total scattering vector q; b) measured (× ×) and calculated (—) Bragg rod intensity profiles $I(q_z)$ of the reflections $\{11\}+\{1\bar{1}\}$, $\{02\}$, and $\{12\}+\{1\bar{2}\}$; c) left, middle: crystalline packing arrangement of the monolayer viewed parallel to the water surface; right: layer packing viewed perpendicular to the water surface.

0947-6539/97/0306-0934 $ 17.50+.50/0 Chem. Eur. J. 1997, 3, No. 6

Quinquethiophene S_5: Samples of S_5 were spread from a very dilute solution of 6.8 μM concentration and measured at nominal areas per molecule of 70, 50, and 35 Å^2 corresponding to a very low surface pressure (see Figure 1b). The obtained GID patterns (Figures 6a, 7a) are consistent with the formation of the β crystalline polymorph (see above section on S_4) composed of molecules aligned normal to the water surface, in a cell of dimensions $a = 5.62$, $b = 7.69$ Å, $\gamma = 90°$. The skewed Bragg peak at $q_{xy} = 1.51$ Å^{-1} observed in one of the samples (Figure 6a) is very similar to that already observed for S_4 spread from very dilute solutions, which was ascribed to an unknown crystalline phase or to an impurity. This peak is inconsistent with the major β polymorph.[21]

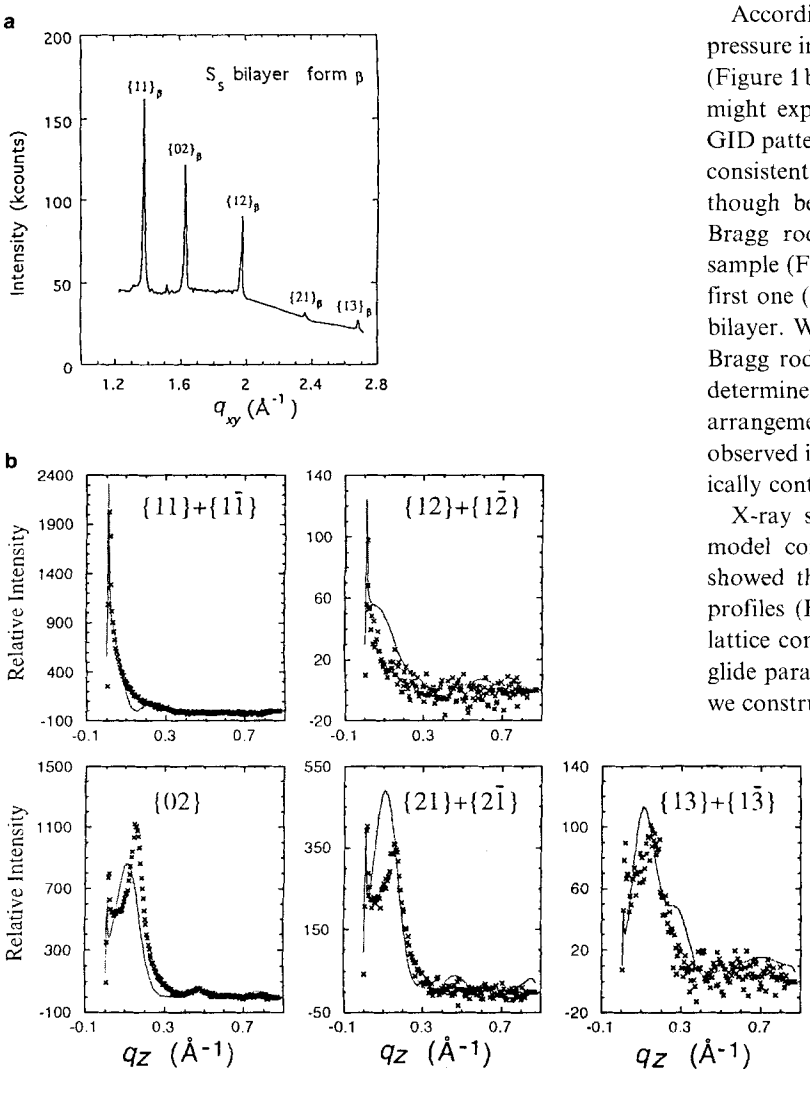

Figure 7. GID results for the bilayer film of S_5 prepared from a spreading solution of 6.8 μM. a) Total scattered intensity $I(q_{xy})$ as a function of the horizontal q_{xy} component of the scattering vector q; b) measured (× ×) and calculated (—) Bragg rod intensity profiles $I(q_z)$ of the reflections $\{11\}+\{1\bar{1}\}$, $\{02\}$, $\{12\}+\{1\bar{2}\}$, $\{21\}+\{2\bar{1}\}$, and $\{13\}+\{1\bar{3}\}$; c) left, middle: crystalline packing arrangement of the bilayer viewed parallel to the water surface; right: layer packing viewed perpendicular to the water surface.

According to the π–A isotherm of S_5, which shows a surface pressure increase starting with an area per molecule of ≈45 Å^2 (Figure 1b, curve b), and the SFM images (Figure 2c), we might expect the formation of a monolayer film. Indeed the GID pattern obtained from one of the S_5 samples (Figure 6b) is consistent with the formation of a crystalline monolayer. Although belonging to the same crystalline β polymorph, the Bragg rod intensity profiles measured from the second S_5 sample (Figure 7b) are very different in shape from that of the first one (Figure 6b), being consistent with the formation of a bilayer. We stress that the distinction between the two sets of Bragg rods (Figures 6b and 7b) is very clear, enabling us to determine unequivocally the crystallites' thickness and packing arrangement. The lack of reproducibility in the number of layers observed indicates that S_5 forms crystalline films under a kinetically controlled process.

X-ray structure factor calculations based on a molecular model constructed from the 3D crystal structure of S_6[19] showed that for the monolayer film the Bragg rod intensity profiles (Figure 6b) are in good agreement with a crystalline lattice constructed of vertically aligned molecules related by a glide parallel to the a axis (Figure 6c). For the bilayer sample, we constructed a crystalline structure of minimum total energy in the space group *Pnam* using CERIUS^2 software.[22] Based on this crystal structure, the calculated Bragg rod intensity profiles (Figure 7b) were obtained for bilayer crystallites, with the molecules being related by glide symmetry (along the a axis) within the layer and by a twofold screw axis (parallel to the c axis) between the layers (Figure 7c). Note that the general shape of the Bragg rods, especially of the high order reflections, is very sensitive to the interlayer packing arrangement, thus enabling us to determine the structure with a high degree of accuracy.

In summary, S_5 forms crystalline monolayer or bilayer self-assemblies at the air–water interface, in a packing arrangement belonging to the β polymorph, namely the untilted form. For the bilayer assemblies, a "three-dimensional" structure with a well-defined space group could be constructed. Whether this β polymorph is induced during crystallization from very dilute spreading solutions, as in the case of the S_4 films, is not clear.

Sexithiophene S_6: The GID measurements were performed on a S_6 film prepared by spreading from a dilute solution (6.9 μM) sonicated for 24 hours because of the very low solubility of the compound, and at nominal areas per molecule of 50 and 25 Å^2 (Figures 8a,b).

We can unambiguously assign the four Bragg peaks at q_{xy} values of 1.378, 1.625, 1.965, and 2.675 Å^{-1} as belonging to a crystalline phase with cell dimensions $a = 5.63$, $b = 7.73$ Å,

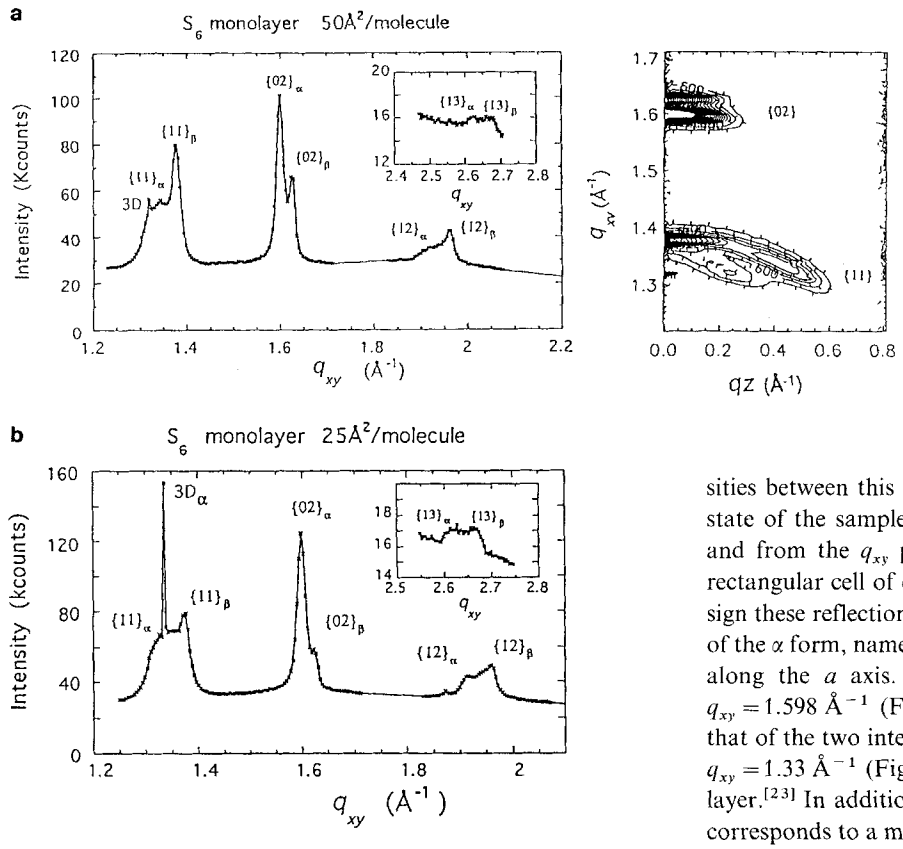

Figure 8. GID results for two points along the $\pi-A$ isotherm of the Langmuir film of S_6 prepared from a spreading solution of 6.9 μM. a) At 50 Å²/molecule: left: total scattered intensity $I(q_{xy})$ as a function of the horizontal q_{xy} scattering vector; right: two-dimensional intensity contour plot $I(q_{xy},q_z)$ as a function of the horizontal q_{xy} and vertical q_z scattering vectors. Note that only $\{11\}+\{1\bar{1}\}$ and $\{02\}$ reflections are shown. b) At 25 Å²/molecule. Scattered intensity $I(q_{xy})$ as a function of the q_{xy} vector. The Bragg peaks of the two polymorphs, abbreviated as α and β, are shown with the corresponding Miller indices. The sharp peak at $q_{xy}=1.31$ Å^{-1} in both a and b, denoted 3D, corresponds to a macroscopic crystal.

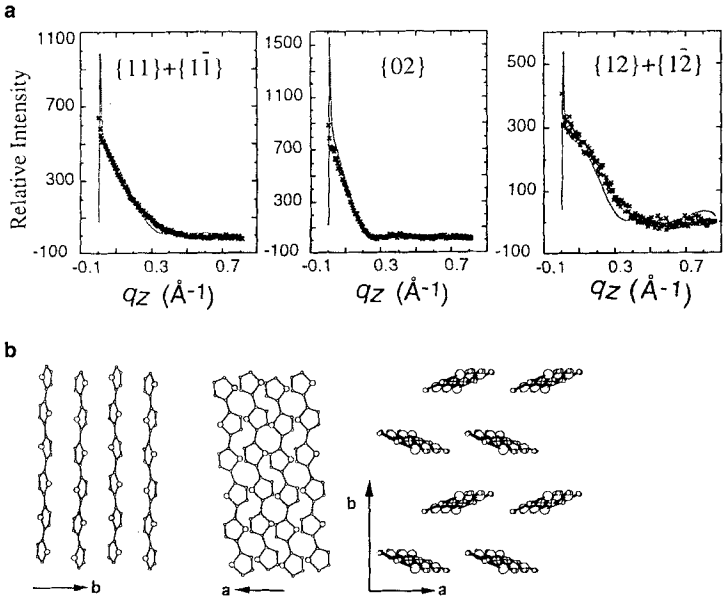

Figure 9. S_6 monolayer crystalline film of the β polymorph: a) measured (× ×) and calculated (–) Bragg rod intensity profiles $I(q_z)$ of the reflections $\{11\}+\{1\bar{1}\}$ and $\{02\}$; b) left, middle: crystalline packing arrangement of the S_6 monolayer viewed parallel to the water surface; right: layer packing viewed perpendicular to the water surface.

$\gamma = 90°$, corresponding to the β form. The film thickness estimated from the Bragg rod profiles corresponds to a monolayer. The packing arrangement of this β form was obtained by construction, with CERIUS[2], of a 2D crystal of minimized lattice energy, with layer symmetry $P2_1/a$ and in which the long molecular axes are aligned perpendicular to the surface. This packing arrangement for a monolayer (Figure 9b) yielded the calculated Bragg rod intensity profiles shown in Figure 9a.

The GID patterns display another set of four Bragg peaks; the ratio of intensities between this set and that of the β phase depends on the state of the sample (Figures 8a,b). Based on this observation and from the q_{xy} positions of all these peaks we obtained a rectangular cell of dimensions $a = 5.9$, $b = 7.86$ Å. We may assign these reflections as belonging to a single phase akin to that of the α form, namely a herringbone structure with chains tilted along the a axis. The FWHM of the $\{0,2\}$ Bragg rod at $q_{xy} = 1.598$ Å^{-1} (Figure 8a, right) suggests a monolayer, but that of the two intensity modulations of the $\{1,1\}$ Bragg rod at $q_{xy} = 1.33$ Å^{-1} (Figure 8a, right) suggests more than a monolayer.[23] In addition, the very narrow peak at q_{xy} of 1.31 Å^{-1} corresponds to a macroscopic crystal of S_6 (α polymorph), presumably not dissolved during the prolonged sonication time, which transiently passed across the beam footprint.

Thus the S_6 films consist mainly of a monomolecular crystalline layer at the air–water interface, in agreement with the $\pi-A$ isotherms and SFM measurements.

Mixed films—sexithiophene as a growth inhibitor: In order to control the thickness of the S_4 self-assemblies, we grew them in the presence of S_6 as a tailor-made growth inhibitor.[24] Since both molecules have very similar structures, S_6 may be incorporated in the S_4 crystallites and perturb their interlayer growth perpendicular to the water surface. Solutions of S_4 (25 μM) containing 10 and 20% (molar) of S_6 were spread at the air–water interface after long

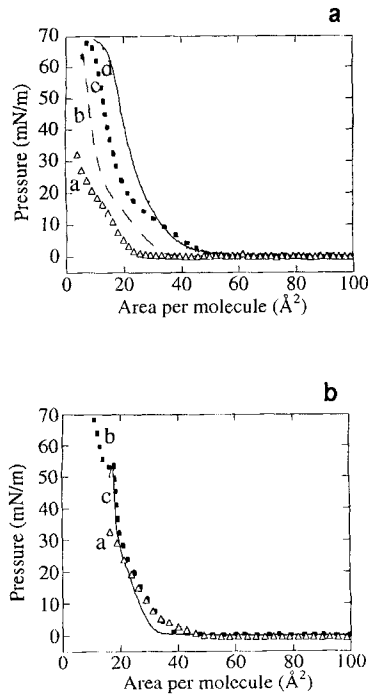

Figure 10. Surface pressure–area isotherms of the mixed films: a) S_4:S_6 with varying percentage of S_6 (a: 0, b: 10, c: 20). The isotherm d of a pure S_6 monolayer film is given as a reference. b) 1:3 S_n:arachidic acid mixed films (a: $n = 4$, b: $n = 6$). The isotherm c of pure arachidic acid monolayer film is given as a reference.

0947-6539/97/0306-0936 $ 17.50+.50/0 Chem. Eur. J. 1997, 3, No. 6

sonication time. The isotherms show a significant increase in the limiting area per molecule, which is 12 and 18 Å^2 respectively (Figure 10a). These values are smaller than those corresponding to a monolayer film, implying that the multilayers were not completely transformed into a monolayer film.

The above conclusion was further supported by Cryo-TEM and SFM measurements on the 10% mixture. The electron diffraction measurements showed a powder pattern composed of rings with *d*-spacings of 4.6, 4.3, 3.8, 3.15, 3.05 Å (not shown). These values could only be explained in terms of a mixture of the two α and β polymorphs. The bright field images exhibit an inhomogeneous membrane differing in morphology from the round domains of the pure S_4. The SFM measurements of this inhomogeneous membrane on the mica support showed formation of a bilayer.

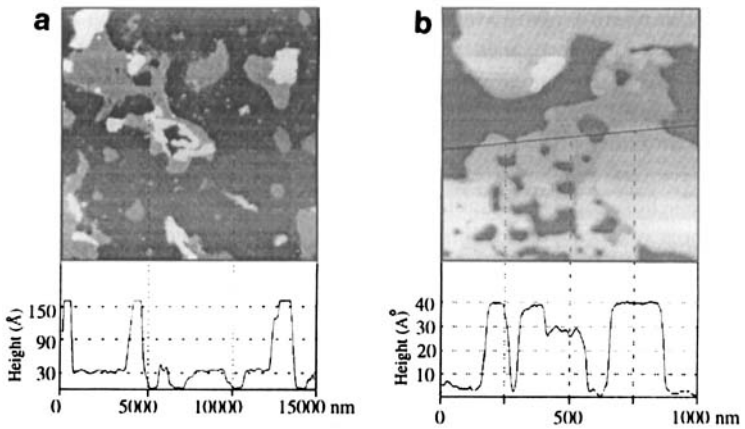

Figure 12. SFM topography images and height profiles of the mixed film: a) 1:3 S_4:arachidic acid; b) 1:3 S_6:tricosanoic acid.

Phase segregation between oligothiophenes and aliphatic acids: Kuhn and coworkers have reported that when S_5 is incorporated inside a thin film of arachidic acid, it operates as a molecular wire that transfers charge from a donor to an acceptor.[24] From the mechanistic viewpoint, it is important to differentiate between charge transfer through isolated molecules or through defined clusters. For this reason, we investigated the structures of the oligothiophenes in mixed films with aliphatic acids.

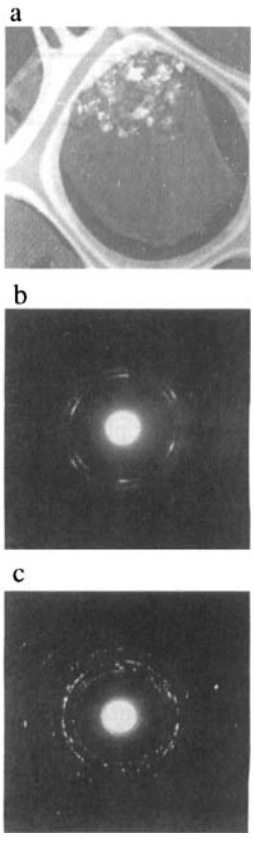

Figure 11. a) Cryo-transmission electron microscopy dark field image of 1:3 S_4:arachidic acid film (scale: 6.5 mm = 1.5 μm); b) electron diffraction pattern of arachidic acid domains inside the mixed film; c) electron diffraction pattern of S_4 domains of the two polymorphs α and β inside the mixed film.

Solutions of 3:1 arachidic acid:S_4 or S_6 (25 μM) were spread at the air-water interface. Their isotherms and that of pure arachidic acid are shown in Figure 10b. The collapse pressure of the S_4 mixture is much lower than those of the pure arachidic acid and of the arachidic acid:S_6 mixture. This observation is consistent with multilayer formation.

The Cryo-TEM bright field images of 3:1 arachidic acid:S_4 exhibit a film in which domains of different contrasts can be observed (Figure 11). The electron diffraction patterns are consistent with phase separation of the two components, showing patterns arising from pure arachidic acid monolayer domains with cell dimensions $a = 4.8$ Å and $b = 7.8$ Å (Figure 11b) and from α and β crystalline domains of pure S_4 (Figure 11c). Similar results were obtained for the arachidic acid:S_6 mixture according to the electron diffraction patterns (not shown).

Phase separation in the various mixtures was also observed by SFM measurements. The height analysis of the arachidic acid:S_4 mixture indicates the presence of regions 250 Å thick, assigned to S_4 multilayers, and regions 30 Å thick corresponding to the arachidic acid monolayer (Figure 12a). The phase separation appears to be general for the oligothiophene:aliphatic acid $C_nH_{2n+1}COOH$ ($n = 19$, 21, 29) mixtures. Differences in thickness between the two phases were monitored by SFM. Figure 12b shows a distinct height of 26 Å corresponding to S_6 domains and about 40 Å corresponding to $C_{29}H_{59}COOH$ domains.

Discussion

We have shown that the oligothiophenes S_4, S_5, and S_6 form crystalline monolayer and multilayer self-assemblies on the water surface. The thickness of the S_5 and S_6 assemblies determined by GID and SFM matched; a monolayer was obtained for S_6, and a monolayer and a bilayer for S_5. For the S_4 molecule, there appears to be an inconsistency. Dilute spreading solution yielded mainly monolayer and some bilayer according to SFM, only bilayer according to GID. The use of a more concentrated solution resulted in formation of thick assemblies, three to ten layers thick according to SFM and $\pi - A$ isotherms, but only a crystalline bilayer judged by GID. We may reconcile this inconsistency in the S_4 study if we assume multilayer formation on the water surface, but with a perfect ordering along the interlayer direction for two layers only, namely a vertical coherence length of two layers, perhaps arising from faults in the stacking of the layers. A similar discrepancy was also noticed in the α,ω-alkanediol[24] and in the *n*-alkane[7] studies. In the alkane system, specular X-ray reflectivity studies support such an interpretation. However, we cannot exclude the possibility of changes in the thickness of the domains during the transfer from the water surface onto the solid support.

According to SFM, comparison of the S_4 samples prepared from concentrated and dilute solutions show much smaller domains from concentrated solution. This result is in keeping with the existence of aggregates in the spreading solution, but not proof thereof. Another piece of evidence suggestive of the presence of aggregates in the spreading solution is the formation of multilayers at high concentration according to SFM. This result

can also be correlated to the shape of the $\pi-A$ isotherms, which are much more expanded for dilute solution and then give an higher average area per molecule. Therefore, the present studies should be also relevant for the understanding of the early stages of crystal nucleation in solution.

Previous studies[25-27] have shown that the orientation (vertical or horizontal) of oligothiophenes evaporated onto a solid support may vary according to the conditions of preparation and the nature of the substrate. The 3D crystal structures of S_4, S_5, and S_6 have layer arrangements in which the molecules adopt a herringbone motif. It is clear that the most dominant molecular interactions lie within the layer. Therefore, strong intralayer interactions should promote the formation of crystalline assemblies with the layer plane parallel to the water, which has indeed been revealed by the various techniques applied, namely GID on water and Cryo-TEM on vitreous ice. The fact that we are able to preserve this orientation after transfer onto a solid support may be of great interest in the construction of conducting devices.

Coexistence of the two polymorphs α and β was observed for S_4 and S_6. The α form, corresponding to the 3D crystal structure of oligothiophenes, consists of molecules with their long axes tilted by about 23° from the direction perpendicular to the layer plane. In the β form of S_4, S_5, and S_6, which has not yet been observed in 3D crystals, the long molecular axis is oriented perpendicular to the layer plane. The (*hk*0) electron diffraction patterns could be simulated from the crystal structures of the two polymorphs (Figures 13a,b) by the CERIUS[2] package. The difference between the two patterns resides mainly in the relative intensities of their electron diffraction spots. These patterns, shown in Figures 13c,d for S_6, display their strongest spots along the reciprocal vectors a^* and b^*, respectively. Based on these simulations, the observed electron diffraction patterns from single crystals S_4 and S_6 (Figures 3b,h) could be unambiguously assigned to the β form. The observed electron diffraction patterns of the partial powder-like film of S_4 (Figure 3b) was interpreted in terms of the presence of both the α and β forms.

The self-assembly of oligothiophenes into crystalline assemblies of molecules aligned perpendicular to the layer plane may be rationalized in terms of favorable lateral interactions within the layer as opposed to weak interactions between the layers. The stability of the two polymorphs was compared by means of lattice energy calculations carried out by CERIUS[2]. The results of the crystal and layer energy calculations, including van der Waals and Coulomb terms from the universal force field, are shown in Table 1 for S_6. Judging by the 3D lattice energy calculations, the two polymorphs are almost equally stable, but in terms of monolayer formation, the β polymorph is the more stable. This result is in agreement with the lattice energy calculation for *n*-alkanes for the monolayer and multilayer formation at the air-water interface.[7]

Table 1. Results of the lattice energy calculations for the two polymorphs of S_6.

S_6 polymorph	Crystal energy (kcal mol^{-1})	Layer energy (kcal mol^{-1})
α	−74.6	−57.0
β	−74.7	−58.4

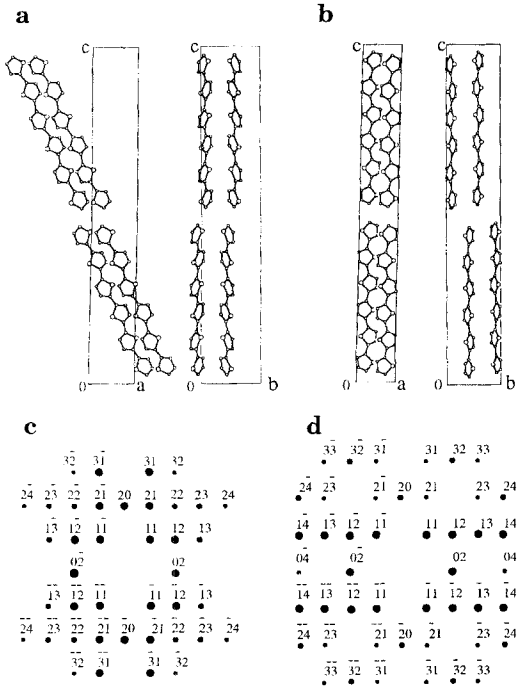

Figure 13. a) Three-dimensional packing arrangement of the α polymorph of S_6 viewed along the *a* and *b* axes; b) simulated three-dimensional packing arrangement of the β polymorph of S_6 viewed along the *a* and *b* axes; c, d) electron diffraction patterns of the α and β polymorphs of S_6 respectively, simulated with CERIUS[2] software.

Conclusion

In this study, we have shown that the formation of crystalline mono- and multilayers on the water surface can be extended from *n*-alkanes to hydrophobic aromatic molecules. The lateral interactions between thiophene rings are strong enough to stabilize two-dimensional crystallinity on the water surface. The results obtained from the various techniques are complementary, although measurements were performed on the water surface, on vitreous ice, and on a mica support. The observed similarities in structure imply that the self-assemblies preserve their crystalline integrity during the transfer from the water surface to a solid support or during the process of freezing. In general, the packing arrangements of the crystallites could be determined to near-atomic resolution from the GID data.

The present study demonstrates that oligothiophene assemblies preserve their structural integrity even when incorporated inside other matrices. A complete phase segregation was observed in the mixed films of oligothiophenes with aliphatic acids. This result might provide a structural insight into the role played by the oligothiophenes as molecular wires.

These results support our previous working hypothesis that in the early stages of crystallisation, clusters of different structures coexist, among which are those adopting a structure akin to that of the 3D macroscopic form. The most stable polymorph will grow at the expense of the metastable ones.[28] This approach has been shown to be useful in the design of tailor-made auxiliaries for the control of crystal polymorphism[29-31] or for the resolution of enantiomers by crystallisation.[32]

0947-6539/97/0306-0938 $ 17.50+.50/0 Chem. Eur. J. 1997, 3, No. 6

Finally, the formation of structured clusters of hydrophobic molecules at the air–liquid interface has been found to be a general phenomenon, and the approach of obtaining ultrathin crystalline films is currently being applied for the formation of supramolecular architectures on solution surfaces.

Acknowledgments: We express our gratitude to Drs. Sidney Cohen and Sophie Matlis for the SFM measurements. S. I. acknowledges a fellowship from the French Ministry of Foreign Affairs. We thank the Minerva Foundation (Munich) and the Israel Academy of Science and Humanity for financial support, and the Danish Foundation for Natural Sciences and Hasylab DESY Hamburg (Germany) for beamtime.

Received: December 18, 1996 [F 550]

[1] G. Horowitz, X. Z. Peng, D. Fichou, F. Garnier, *J. Mol. Electron.* **1991**, *7*, 85.
[2] A. Dodabalapur, L. Torsi, H. E. Katz, *Science* **1995**, *268*, 270.
[3] E. E. Polymeropoulos, D. Mobius, H. Kuhn, *J. Chem. Phys.* **1978**, *68*, 3918.
[4] N. Theophilou, D. B. Swanson, A. G. MacDiarmid, A. Chakraborty, H. H. S. Javadi, S. P. Treat, F. Zuo, A. J. Epstein, *Synth. Metals* **1989**, *21*, D35.
[5] S. Hotta, K. Waragai, *Adv. Mater.* **1993**, *5*, 896.
[6] M. Y. Li, A. A. Acero, Z. Q. Huang, S. A. Rice, *Nature* **1994**, *367*, 151.
[7] S. P. Weinbach, I. Weissbuch, K. Kjaer, W. G. Bouwman, J. Als-Nielsen, M. Lahav, L. Leiserowitz, *Adv. Mater.* **1995**, *7*, 857.
[8] K. Tamao, S. Kodama, I. Nakajima, M. Kumada, A. Minato, K. Suzuki, *Tetrahedron* **1982**, *38*, 3347.
[9] D. Fichou, G. Horowitz, F. Garnier, *Eur. Pat. Appl. EP402269*, **1990** (*Chem. Abstr. 114*, 186387g).
[10] A. Schaper, L. Wolthaus, D. Mobius, T. M. Jovin, *Langmuir* **1993**, *9*, 2178.
[11] J. Majewski, L. Margulis, I. Weissbuch, R. Popovitz-Biro, T. Arad, Y. Arad, M. Lahav, L. Leiserowitz, *Adv. Mater.* **1995**, *7*, 26.
[12] J. Als-Nielsen, D. Jacquemain, K. Kjaer, F. Leveiller, M. Lahav, L. Leiserowitz, *Phys. Rep.* **1994**, *246*, 251.
[13] J. Majewski, R. Popovitz-Biro, W. G. Bouwman, K. Kjaer, J. Als-Nielsen, M. Lahav, L. Leiserowitz, *Chem. Eur. J.* **1995**, *1*, 304.
[14] D. Jacquemain, S. Grayer Wolf, F. Leveiller, M. Deutsch, K. Kjaer, J. Als-Nielsen, M. Lahav, L. Leiserowitz, *Angew. Chem. Int. Ed. Engl.* **1992**, *31*, 130.
[15] J. Majewski, L. Margulis, D. Jacquemain, F. Leveiller, C. Bohm, T. Arad, Y. Talmon, M. Lahav, L. Leiserowitz, *Science* **1993**, *261*, 891.
[16] W. Porzio, S. Destri, M. Mascherpa, S. Bruckner, *Acta Polym.* **1993**, *44*, 266.
[17] The thickness of the crystalline film was first derived from the full width at half maximum (FWHM) of the two intensity modulations of the $\{11\}+\{1\bar{1}\}$ Bragg rods at $q_z \approx 0.19$ Å^{-1} and $q_z \approx 0.56$ Å^{-1}, yielding a FWHM of 0.17 Å and so a thickness of $0.9 \times 2\pi/0.17 = 33$ Å.
[18] The contour lines of the intensity distribution $I(q_{xy},q_z)$ at the $\{1,1\}$ reflection are skewed (not shown), extending along Scherrer rings given by $(q_{xy}^2 + q_z^2)$ = constant. An analysis of the shape of the peak yields a film thickness of 38 Å, corresponding to 2–3 layers: K. Kjaer, W. G. Bouwmann, *Annual Progress Report of the Department of Solid State Physics* (Eds: P. A. Lindgaard, K. Bechgaard, K. N. Clausen, R. Feidenhans'l), Risø National Laboratory, Roskilde (Denmark), **1995**, p. 79.
[19] G. Horowitz, B. Bachet, A. Yassar, P. Lang, F. Demanze, J. L. Fave, F. Garnier, *Chem. Mater.* **1995**, *7*, 1337.
[20] D. Fichou, B. Bachet, F. Demanze, I. Billy, G. Horowitz, F. Garnier, *Adv. Mater.* **1996**, *8*, 500.
[21] On one hand we may assign this peak to an impurity, since it was also observed for the S_4 film obtained from dilute spreading solution that was prepared from the same chloroform solvent bottle. On the other hand, if the peak belongs to a crystalline phase originating from the S_5 amphiphile, the assignment of the peak at $q_{xy} = 1.516$ Å^{-1} yields a hexagonal phase $a = b = 4.8$ Å^2, $\gamma = 120°$, which is unreasonable in terms of the low area per molecule of 20.05 Å^2. If we combine this reflection with the weak unassigned peak at 1.69 Å to form a rectangular cell, the area per molecule is once again too low. We did not assign it, and when the experiment was repeated we obtained a bilayer of β phase, with no indication of the skewed peak.
[22] CERIUS^2: molecular modeling software for materials research, Molecular Simulations, Burlington MA (USA) and Cambridge (UK).
[23] The contours of these two modulations are skewed in a way that we cannot explain: the skewness is not along the Scherrer rings of constant $q_i^2 = q_{xy}^2 + q_z^2$. The presence of the two modulations is somewhat similar to that observed in the α form of S_4 (Figure 4b). However, the separation between the maxima of the two modulations along q_z yields an "interlayer" spacing of ≈ 27 Å, which is about 5 Å longer than the corresponding interlayer spacing in the 3D crystal of S_6 that appears in the α form.
[24] R. Popovitz-Biro, J. Majewski, L. Margulis, S. Cohen, L. Leiserowitz, M. Lahav, *Adv. Mater.* **1994**, *6*, 956.
[25] B. Servet, G. Horowitz, S. Ries, O. Lagorsse, P. Alnot, A. Yassar, F. Deloffre, P. Srivastava, R. Hajlaoui, P. Lang, F. Garnier, *Chem. Mater.* **1994**, *6*, 1809.
[26] O. Böhme, C. Ziegler, W. Göpel, *Adv. Mater.* **1994**, *6*, 587.
[27] P. Bäuerle, T. Fischer, B. Bidlingmeier, A. Stabel, J. P. Rabe, *Angew. Chem. Int. Ed. Engl.* **1995**, *34*, 303.
[28] I. Weissbuch, I. Kuzmenko, M. Vaida, S. Zait, L. Leiserowitz, M. Lahav, *Chem. Mater.* **1994**, *6*, 1258.
[29] I. Weissbuch, D. Zbaida, L. Addadi, M. Lahav, L. Leiserowitz, *J. Am. Chem. Soc.* **1987**, *109*, 1869.
[30] E. Staab, L. Addadi, L. Leiserowitz, M. Lahav, *Adv. Mater.* **1990**, *2*, 40.
[31] I. Weissbuch, L. Leiserowitz, M. Lahav, *Adv. Mater.* **1994**, *6*, 952.
[32] D. Zbaida, I. Weissbuch, E. Shavit-Gati, L. Addadi, L. Leiserowitz, M. Lahav, *React. Polym.* **1987**, *6*, 241.

  0947-6539/97/0306-0939 $ 17.50+.50/0